

Article

Cavitation Limits the Recovery of Gas Exchange after Severe Drought Stress in Holm Oak (*Quercus ilex* L.)

José Javier Peguero-Pina, Óscar Mendoza-Herrer, Eustaquio Gil-Pelegrín * and Domingo Sancho-Knapik

Unidad de Recursos Forestales, Centro de Investigación y Tecnología Agroalimentaria de Aragón, Gobierno de Aragón, Avda. Montañana 930, 50059 Zaragoza, Spain; jipeguero@aragon.es (J.J.P.-P.); oscarmendozaherrer@gmail.com (Ó.M.-H.); dsancho@cita-aragon.es (D.S.-K.)

* Correspondence: egilp@aragon.es; Tel.: +34-976-716-394

Received: 12 July 2018; Accepted: 23 July 2018; Published: 24 July 2018



Abstract: Holm oak (*Quercus ilex* L.) is a Mediterranean species that can withstand intense summer drought through a high resistance to cavitation far beyond the stomatal closure. Besides stomatal limitations, both mesophyll and biochemical limitations to CO₂ uptake could increase in holm oak under drought. However, no studies have addressed how hydraulic and non-hydraulic factors may limit the recovery of photosynthesis when re-watering after inducing 50% loss of hydraulic conductivity. We measured photosynthetic traits, xylem embolism, and abscisic acid (ABA) in holm oak with increasing levels of drought stress and seven days after plant re-watering. Drought stress caused a sharp decrease in net CO₂ assimilation (A_N), stomatal and mesophyll conductance (g_s and g_m), and maximum velocity of carboxylation (V_{cmax}). The stomatal closure could be mediated by the rapid increase found in ABA. The high level of xylem embolism explained the strong down-regulation of g_s even after re-watering. Therefore, only a partial recovery of A_N was observed, in spite of non-hydraulic factors not limiting the recovery of A_N , because i/ABA strongly decreased after re-watering, and ii/g_m and V_{cmax} recovered their original values. Therefore, the hydraulic-stomatal limitation model would be involved in the partial recovery of A_N , in order to prevent extensive xylem embolism under subsequent drought events that could compromise holm oak survival.

Keywords: abscisic acid; drought; holm oak; maximum velocity of carboxylation; mesophyll conductance; photosynthesis; recovery; stomatal conductance; xylem embolism

1. Introduction

Mediterranean-type climates are characterized by hot/dry summers and mild or cold winters that can potentially restrict vegetative activity [1,2]. This type of climate is found in several regions between 30° and 40° latitude on the western sides of continents [3], in areas where the shift of the subtropical high pressure cells to higher latitudes during summer causes atmospheric stability, and as a consequence, an absence of rainfall [4]. Moreover, climate change projections indicate that Mediterranean ecosystems could experience drastic reductions in precipitation that will exacerbate seasonal drought stress [5,6]. Therefore, plant species growing in the Mediterranean area should develop mechanisms and strategies to cope with prolonged periods of water shortage [7].

Stomatal closure in response to drought is a common way of regulating water consumption [8–11]. This strategy is considered to be an effective mechanism that prevents xylem cavitation and runaway embolism [12,13], albeit at the expense of a reduction in net CO₂ assimilation that could compromise the carbon balance of the plant [2,14]. The existence of a delay between the water potential leading stomatal closure and that inducing extensive xylem cavitation (i.e., a wide “security margin”) [15] is common in plants occurring in water-limited environments [16]. Several studies suggest that a

wide “security margin” would increase the survival and competitiveness under Mediterranean severe drought conditions [12,17].

Holm oak (*Quercus ilex* L.) is a keystone Circum-Mediterranean tree species—both in terms geographic distribution and landscape dominance—that experiences very negative water potentials under extreme drought (a more anisohydric behavior) [18], and shows high resistance to drought-induced cavitation [19]. This species has a wide “security margin” because stomatal closure occurs at water potentials (ca. -3 MPa) [10,12] much higher than those inducing 50% Loss of Hydraulic Conductivity (PLC₅₀) (ca. -6 MPa) [19]. Despite this, in periods of extended drought, stomatal closure cannot sufficiently restrict water loss to prevent the formation of extensive embolism in the xylem [20].

Besides stomatal limitations, drought stress can also reduce photosynthesis by (i) decreasing the mesophyll conductance to CO₂ (g_m), i.e., increasing the CO₂ transfer resistance from intercellular air spaces to carboxylation sites in chloroplasts (mesophyll limitations), and (ii) decreasing the maximum carboxylase activity of Rubisco (V_{cmax}), i.e., inhibiting the capacity to fix CO₂ into sugars (biochemical limitations) [21]. Regarding holm oak, Galle et al. [22] showed evidence that mesophyll limitations increased when experiencing drought stress; this plays a predominant role in limiting photosynthesis under these conditions. Moreover, these authors also characterized the velocity of recovery of photosynthetic traits after re-watering, but they only found a partial recovery of net CO₂ assimilation due to persistently low stomatal and mesophyll conductances.

The time to recovery of plant function is critical for ecosystem function, especially if a new drought arrives, as was recently addressed by Schwalm et al. [23]. However, few studies have addressed the relationship between hydraulic and photosynthetic traits during drought and recovery [20,24–27]. Overall, these authors suggested that recovery of photosynthetic capacity could be driven by recovery of ability for water transport to the transpiring leaves. Besides hydraulic traits, Yan et al. [28] proposed that non-hydraulic factors might jeopardize the recovery of gas exchange from severe drought in *Robinia pseudoacacia*, i.e., through the existence of residual abscisic acid (ABA) during the recovery stage.

However, to the extent of our knowledge, no studies have addressed the role of both hydraulic (xylem embolism) and non-hydraulic factors (namely g_m , V_{cmax} and ABA) in the decline of the photosynthetic activity of holm oak under severe drought conditions, and its subsequent recovery after re-watering, which is the main objective of the present study. We hypothesized that recovery of net CO₂ assimilation in holm oak after imposing a severe drought (i.e., reaching water potential values close to PLC₅₀) would be compromised by extensive xylem embolism, more than by non-hydraulic factors.

2. Materials and Methods

2.1. Plant Material and Experimental Conditions

Seeds from holm oak (*Q. ilex* subsp. *rotundifolia*) (“Soria” provenance, 41°46′ N, 2°29′ W, 1074 m above sea level, Spain) were sown and cultivated in 2003 in 0.5 L containers inside a greenhouse under the same conditions with a mixture of 80% compost (Neuhaus Humin Substrat N6; Klasman-Deilmann GmbH, Geeste, Germany) and 20% perlite. After the first growth cycle, the seedlings were transplanted to 25 L containers filled with the same mixture of compost and perlite, and cultivated outdoors at CITA de Aragón (41°39′ N, 0°52′ W, Zaragoza, Spain), under Mediterranean conditions (mean annual temperature 15.4 °C, total annual precipitation 298 mm). A slow-release fertilizer (15:9:12 N:P:K, Osmocote Plus, Sierra Chemical, Milpitas, CA, USA) was periodically added to the top 10-cm layer of substrate (3 g L⁻¹ growth substrate). All plants were grown under the same environmental conditions, drip-irrigated every 2 days and pruned when necessary.

Two weeks before the beginning of the experiment, ten potted plants (14-years-old and ca. 1.5 m in height and ca. 0.8 m of maximum diameter) were placed under a clear plastic roof (polyethylene film for greenhouse covering, 200 μm thickness) that allowed the passing 90% of PPFD (~1800 μmol photons m⁻² s⁻¹ at midday, during the experiment). The use of covers in water-stress experiments had the advantage of performing measurements in more controlled environmental conditions, i.e.,

avoiding re-watering by storms or unwanted rainfall events. Watering was stopped on 21 August 2017, and measurements in well-watered plants started on 22 August 2017. Over the following days, measurements were performed in the same plants every two or three days with increasing levels of drought stress. Drought stress was imposed during 20 days. Finally, after the last measurement under drought stressed conditions, plants were re-watered, and measurements were performed again after 7 days.

Air temperature (T, °C) and relative humidity (RH, %) were measured at the experimental site using a Hobo Pro temp/RH data logger (Onset Computer, Bourne, MA, USA) located at 1.30 m above the soil surface. Measurements were recorded every 60 min from June to September of 2017. Vapour pressure deficit (VPD, kPa) was calculated from values of T and RH according to Rundel and Jarrell [29]. Mean and maximum diurnal (from dawn to sunset) VPD values for this period are shown in Figure S1.

2.2. Water Potential Measurements

Predawn and midday leaf water potentials (ψ_{PD} and ψ_{MD} , MPa) were measured in shoots of holm oak (with leaves still attached to the shoots) with a Scholander pressure chamber following the methodological procedure described by Turner [30].

2.3. Leaf Gas Exchange and Chlorophyll Fluorescence Measurements

Simultaneous gas-exchange and chlorophyll fluorescence measurements were conducted with an open gas exchange system (CIRAS-2, PP-Systems, Amesbury, MA, USA) fitted with an automatic universal leaf cuvette (PLC6-U, PP-Systems) and an FMS II portable pulse amplitude modulated fluorometer (Hansatech Instruments Ltd., Norfolk, UK). All measurements were performed between 8 and 9 h (solar time) in fully developed current-year attached leaves of holm oak, at controlled cuvette CO₂ concentration ($C_a = 400 \mu\text{mol mol}^{-1}$) and a saturating photosynthetic photon flux density (PPFD) of $1500 \mu\text{mol m}^{-2} \text{s}^{-1}$. In all measurements, the vapor pressure deficit was kept at 1.25 kPa, and leaf temperature at 25 °C. After steady-state gas-exchange was reached, net CO₂ uptake (A_N , $\mu\text{mol CO}_2 \text{m}^{-2} \text{s}^{-1}$), stomatal conductance (g_s , $\text{mmol H}_2\text{O m}^{-2} \text{s}^{-1}$) and the effective quantum yield of PSII (Φ_{PSII}) were estimated. The Φ_{PSII} was calculated as $(F'_M - F_S)/F'_M$, where F_S is the steady-state fluorescence and F'_M is the maximum fluorescence during a light-saturating pulse of $\sim 8000 \mu\text{mol m}^{-2} \text{s}^{-1}$ [31]. Photosynthetic electron transport rate (J_F) was then calculated according to Krall and Edwards [32], following the methodology described in Peguero-Pina et al. [33]. Leakage of CO₂ in and out of the cuvette was determined as described in Flexas et al. [34], and used to correct for measured leaf fluxes.

Mesophyll conductance (g_m) and maximum velocity of carboxylation (V_{cmax}) were estimated according to the method of Harley et al. [35] (Equation (1)), and the one-point method of De Kauwe et al. [36] Equation (2), respectively, as follows:

$$g_m = \frac{A_N}{C_i - \frac{\Gamma^*(J_F + 8(A_N + R_L))}{J_F - 4(A_N + R_L)}} \quad (1)$$

$$V_{cmax} = \frac{A_N}{\left(\frac{C_i - \Gamma^*}{C_i + K_m}\right) - 0.015} \quad (2)$$

where A_N and the substomatal CO₂ concentration (C_i) were taken from the gas-exchange measurements at saturating light. The chloroplastic CO₂ compensation point in the absence of mitochondrial respiration (Γ^*) and the respiration rate in the light (R_L) were estimated as described in Flexas et al. [37], whereas K_m (the Michaelis-Menten constant) was estimated as described in De Kauwe et al. [36].

To separate the relative controls on A_N resulting from limited stomatal conductance (l_s), mesophyll diffusion (l_m) and biochemical capacity (l_b), we used the quantitative limitation analysis of Grassi

and Magnani [38], as applied in Tomás et al. [39] and Peguero Pina et al. [40]. Different fractional limitations, l_s , l_m and l_b ($l_s + l_m + l_b = 1$) were calculated as:

$$l_s = \frac{g_{\text{tot}}/g_s \cdot \delta AN_N / \delta C_c}{g_{\text{tot}} + \delta AN_N / \delta C_c} \quad (3)$$

$$l_m = \frac{g_{\text{tot}}/g_m \cdot \delta AN_N / \delta C_c}{g_{\text{tot}} + \delta AN_N / \delta C_c} \quad (4)$$

$$l_b = \frac{g_{\text{tot}}}{g_{\text{tot}} + \delta AN_N / \delta C_c} \quad (5)$$

where g_s is the stomatal conductance to CO_2 , g_m is the mesophyll conductance according to Harley et al. [35] Equation (1), and g_{tot} is the total conductance to CO_2 from ambient air to chloroplasts (sum of the inverse CO_2 serial conductances g_s and g_m). The values of g_m obtained were used to calculate the chloroplastic CO_2 concentration (C_c) using the equation $C_c = C_i - A_N/g_m$.

2.4. Whole-Plant Transpiration and Conductance

Whole-plant transpiration was estimated through lysimetric measurements by weighing the plant pots from the early morning to midday every 2 h (6, 8, 10 and 12 h solar time) with a precision balance (Wagi Load Cell WLC 20/A2, Radwag Balances and Scales, Radom, Poland). In order to consider only the water losses by plant transpiration, the surface of the ground and the pot drain holes were sealed before the first measurement; these seals were removed after the last measurement of the day. Transpiration ($\text{mol H}_2\text{O s}^{-1}$) was calculated as the difference in weight divided by the time lapse between two consecutive measurements. Whole-plant transpiration on leaf area basis (E_{plant} , $\text{mol H}_2\text{O m}^{-2} \text{s}^{-1}$) was calculated by estimating total leaf area per plant; to do this, single leaf area was estimated in 20 representative leaves per plant and the total number of leaves per plant was quantified. Moreover, whole-plant conductance (g_{plant}) was derived from Ficks law of diffusion, as described in Pearcy et al. [41]:

$$g_{\text{plant}} = \frac{E_{\text{plant}}}{\Delta VPD} \quad (6)$$

where ΔVPD is the leaf-air vapour pressure difference.

2.5. Native Xylem Embolism

Native xylem embolism was estimated in current-year twigs of holm oak collected from branches where ψ_{MD} had previously been measured. The twigs were cut under water in the field and immediately carried out to the lab in a plastic bag. Once there, the stem segments of the twigs were cut under water again (50 mm long), and both ends were shaved with a razor blade. The segments were placed in a tubing similar to that described by Cochard et al. [42] and connected to a digital mass flowmeter Liqui-Flow (Bronkhorst High-Tech, Ruurlo, The Netherlands). The tubing with the twigs was immersed in distilled water to prevent desiccation and to maintain a near constant temperature [12]. The segments were perfused with distilled, degassed and filtered (0.22 μm) water containing 0.005% (v/v) Micropur (Katadyn Products, Wallisellen, Switzerland) to prevent microbial growth [43]. The hydraulic conductivity was measured before and after removing air embolisms by applying short perfusions at 0.15 MPa for 60–90 s, as described by Sperry et al. [44]. Native embolism was then calculated as the ratio between the hydraulic conductivity before and after removing embolism.

2.6. Abscisic Acid Determination

Abscisic acid (ABA) was determined in current-year fully developed leaves of holm oak. Samples were collected at midday and stored at -80°C for preservation until analysis. Fifty milligrams of lyophilized tissue was extracted twice with 3 mL of acetone/water/formic acid (80:19:1, $v/v/v$) (30 min,

2000 rpm) and centrifuged (15 min, 3000 rpm, 4 °C). The acetone was evaporated under a nitrogen stream, and the remaining aqueous extract was adjusted to 1.2 mL with Milli-Q water. The extract was partitioned twice with diethyl ether, dried under nitrogen, and redissolved in 500 μ L acetonitrile/water (30:70, *v/v*) containing 0.1% formic acid. The extract was analyzed by mass spectrometry, and ABA was quantified following the methodology described in Sancho-Knapik et al. [45].

2.7. Statistical Analysis

Data are expressed as means \pm standard error. One-way ANOVAs were performed to identify the effect of time of measurement on whole-plant transpiration (E_{plant}) and conductance (g_{plant}). Multiple comparisons were carried out among times of measurement for E_{plant} and g_{plant} using the post hoc Tukey's Honest Significant Difference test. Student's *t*-tests were used to compare the values of photosynthetic traits (A_N , g_s , g_m and V_{cmax}) measured for well-watered plants before the drought period with those measured 7 days after plants were rewatered. All statistical analyses were performed with SAS version 8.0 (SAS, Cary, NC, USA).

3. Results

3.1. Whole-Plant Transpiration and Conductance

Both transpiration and conductance at whole-plant level (E_{plant} and g_{plant}) decreased in holm oak when predawn water potential (ψ_{PD}) became more negative (Figure 1). At the end of the drought period (when ψ_{PD} was ca. -6 MPa), both E_{plant} and g_{plant} reached almost negligible values. E_{plant} for well-watered plants was statistically higher at midday (solar time) when compared with the values obtained in early- and mid-morning (Figure 1a). This fact can be explained by the gradual increase in VPD from early morning to midday because g_{plant} did not show differences among different times of measurement for well-watered plants (when ψ_{PD} was ca. 0 MPa, Figure 1b). g_{plant} only showed differences among different times of measurement when ψ_{PD} was ca. -3 MPa.

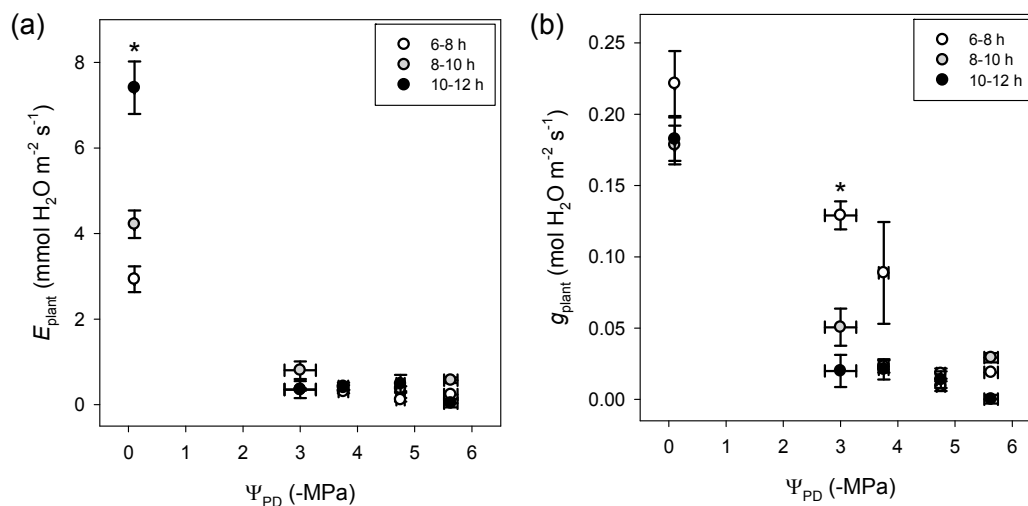


Figure 1. Time course of (a) whole-plant transpiration (E_{plant}) and (b) whole-plant conductance (g_{plant}) with predawn water potential (ψ_{PD}) for holm oak leaves during the drought period at early morning (between 6 and 8 h solar time, white symbols), mid-morning (between 8 and 10 h solar time, grey symbols) and midday (between 10 and 12 h solar time, black symbols). Data are mean \pm SE. Asterisks indicate significant differences among early morning, mid-morning and midday for each level of ψ_{PD} (Tukey's test, $p < 0.05$).

3.2. Photosynthetic Traits at Leaf Level

Both net photosynthesis and stomatal conductance at leaf level (A_N and g_s) decreased in holm oak when ψ_{PD} became more negative, reaching negative values for A_N and almost negligible values for g_s at the end of the drought period (Figure 2), which agreed with the results obtained at the whole-plant level (Figure 1). Both A_N and g_s showed a partial recovery when plants were re-watered, although this was much higher for A_N than for g_s (64% and 29% with respect to the values for well-watered plants, respectively). This pattern was also observed for mesophyll conductance and maximum velocity of carboxylation (g_m and V_{cmax}), which showed a sharp decrease throughout the drought period (Figure 3). However, contrary to g_s , the recovery of g_m and V_{cmax} was almost complete 7 days after plants were re-watered (89 and 75%, respectively).

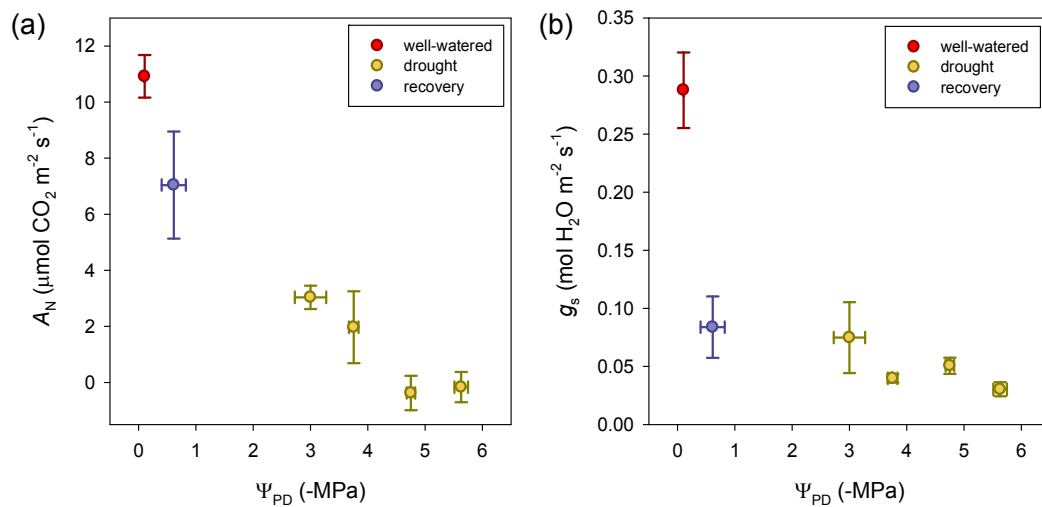


Figure 2. Time course of (a) net photosynthesis (A_N) and (b) stomatal conductance (g_s) with predawn water potential (ψ_{PD}) for holm oak leaves well-watered (red symbols), during the drought period (yellow symbols) and 7 days after plants were re-watered (violet symbols). Data are mean \pm SE.

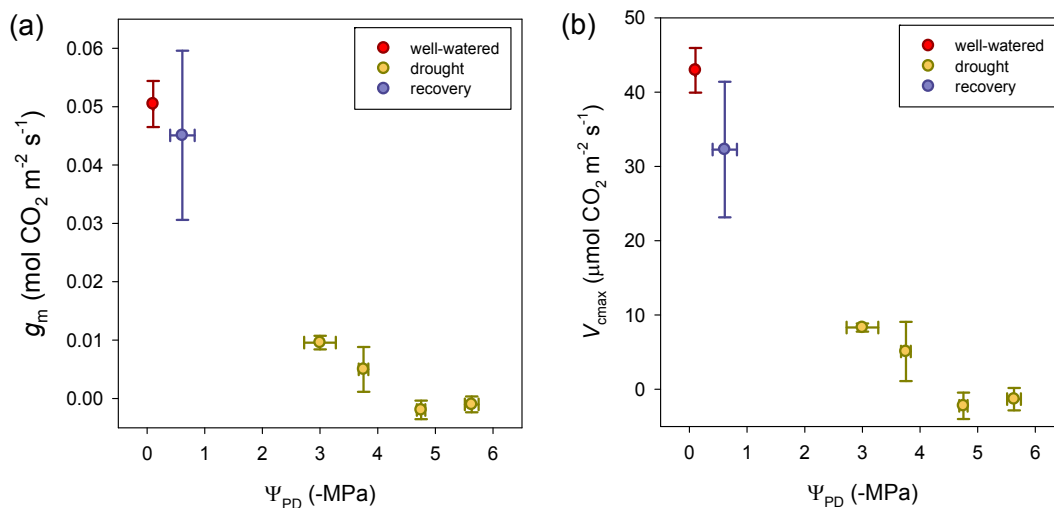


Figure 3. Time course of (a) mesophyll conductance (g_m) and (b) maximum velocity of carboxylation (V_{cmax}) with predawn water potential (ψ_{PD}) for holm oak leaves well-watered (red symbols), during the drought period (yellow symbols) and 7 days after plants were re-watered (violet symbols). Data are mean \pm SE.

The analysis of the partitioning of photosynthetic limitations revealed that A_N was mainly limited by mesophyll conductance (l_m) for well-watered plants, which was gradually increased during the drought period (Figure 4). However, there was a strong increase in l_s and a strong decrease in l_m 7 days after plants were re-watered (Figure 3), probably associated with the lack of recovery in g_s (Figure 2).

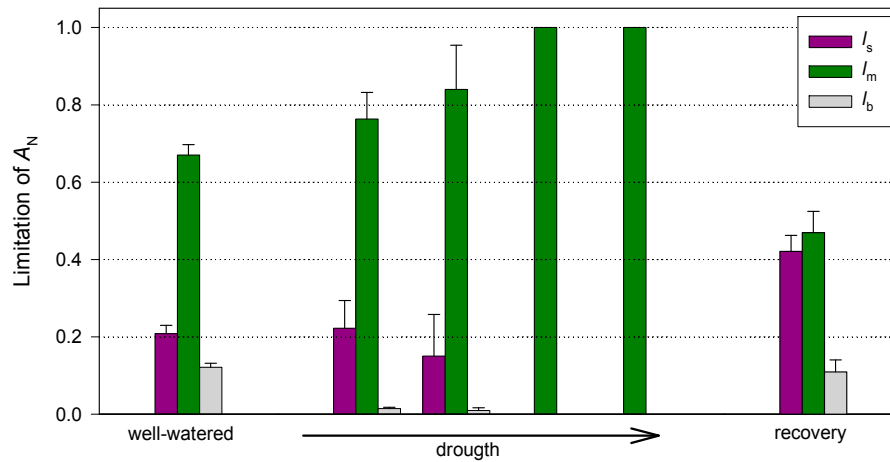


Figure 4. Relative stomatal (l_s), mesophyll (l_m) and biochemical (l_b) photosynthesis limitations for holm oak leaves well-watered, with increasing levels of drought stress and 7 days after plants were re-watered. Data are mean \pm SE.

3.3. Native Xylem Embolism

The increasing levels of maximum daily drought stress (estimated through the measurement of ψ_{MD}) induced a progressive loss of hydraulic conductivity in holm oak twigs, reaching values of native xylem embolism ca. 50% at the end of the drought period. This value of native embolism remained almost constant for 7 days after plants were re-watered (ca. 55%, Figure 5).

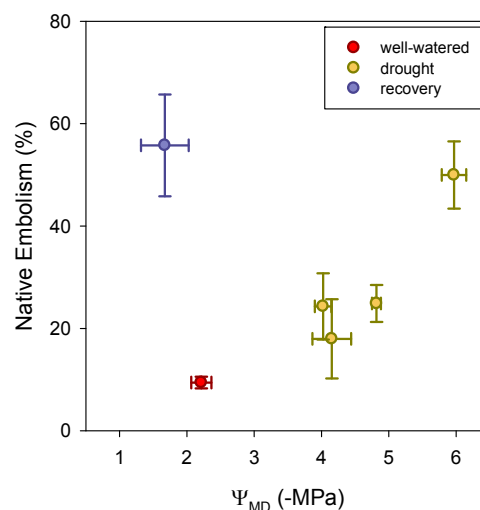


Figure 5. Time course of native xylem embolism (%) with midday water potential (ψ_{MD}) for holm oak twigs well-watered (red symbols), during the drought period (yellow symbols) and 7 days after plants were re-watered (violet symbols). Data are mean \pm SE.

3.4. Abscisic Acid

The increasing levels of drought stress induced a sharp increase in ABA concentration, reaching maximum values at ψ_{PD} between -3 and -4 MPa (Figure 6). Despite ABA progressively decreasing

until the end of the drought period, the residual value after plants were re-watered was much lower than that registered throughout the drought period, but slightly higher than that for well-watered plants (Figure 6).

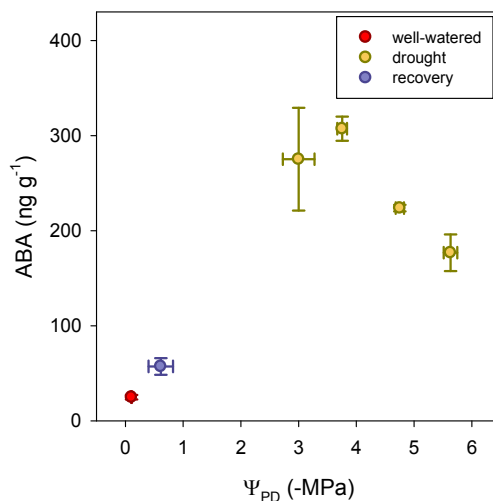


Figure 6. Time course of abscisic acid (ABA, ng g⁻¹) with predawn water potential (ψ_{PD}) for well-watered holm oak leaves (red symbols) during the drought period (yellow symbols) and 7 days after plants were re-watered (violet symbols). Data are mean \pm SE.

4. Discussion

4.1. Drought Period

All the photosynthetic traits analyzed for holm oak leaves showed strong reductions when increasing the levels of drought, reaching almost negligible values at the end of the drought period (Figures 2 and 3). Thus, the ability for net CO₂ uptake (A_N) was progressively decreased and became negative when predawn water potential (ψ_{PD}) was ca. -5 MPa, as previously reported for this species [10]. The drop experienced by A_N throughout the drought period was accompanied by strong reductions for the rest of photosynthetic traits, i.e., stomatal conductance (g_s), mesophyll conductance (g_m), and maximum velocity of carboxylation (V_{cmax}). These results indicate that both diffusive (stomatal and mesophyll) and non-diffusive (biochemical) limitations of photosynthesis increased throughout the drought period, which helped explain the pattern followed by A_N . Regarding to this, Galle et al. [22] reported a similar performance for A_N , g_s and g_m in holm oak when subjected to drought, although these authors found that V_{cmax} was not affected throughout the experiment.

Regardless of the absolute increase found for all the factors potentially limiting photosynthesis, the analysis of the partitioning of the different components revealed that g_m was the most limiting factor for net CO₂ assimilation for well-watered plants and throughout the drought period (Figure 4), which confirms the important role of g_m in the photosynthetic capacity of holm oak [46]. In fact, the relative importance of mesophyll limitation (l_m) was gradually increased during the drought period, from 0.67 for well-watered plants up to 1.00 when ψ_{PD} was ca. -5 MPa (Figure 4), concurrently with the point when A_N became negative (Figure 2).

Besides g_m , the response found in g_s under drought stress also imposed a strong limitation to CO₂ uptake. As stated in the Introduction, this is a common mechanism in Mediterranean plants in response to a reduction in soil water availability that has been reported for holm oak [10]. The results found in the present study seem to indicate that the stomatal closure at the onset of the drought period (when ψ_{PD} was ca. -3 MPa) could be driven by the rapid increase in abscisic acid (ABA) (Figure 6), a plant hormone that initiates a signaling cascade to close stomata and reduce water loss [47]. It should be noted that, at this stage, a down-regulation of stomatal conductance at whole-plant level (g_{plant})

from the early morning to midday (Figure 1) was also detected, probably associated to hydraulic factors due to the effect of incipient xylem embolism (Figure 6). Afterwards, ABA concentration showed a slight decline until the end of the drought period, as observed by Yan et al. [28] for *Amorpha fruticosa* and *Robinia pseudoacacia*. Furthermore, the results derived from this work provide evidence that even an almost complete stomatal closure (i.e., g_s below $0.030 \text{ mol H}_2\text{O m}^{-2} \text{ s}^{-1}$) cannot impede a meaningful loss of hydraulic conductivity in the xylem (ca. 50% at the end of the drought period, Figure 5).

4.2. Recovery

The values of ψ_{PD} for holm oak recovered from -5.6 MPa at the end of the drought period to -0.6 MPa 7 days after re-watering, although this value was slightly more negative than that for well-watered plants (-0.1 MPa). The rate of recovery of the different photosynthetic traits showed meaningful differences among them. Thus, g_m and V_{cmax} recovered the original values registered for well-watered plants (Figure 3, Table 1), which is in accordance with the results showed by Galle et al. [22] for holm oak. However, contrary to our findings, these authors reported that A_N and g_s in holm oak restored the control values even after three drought cycles. In fact, we observed only a partial recovery of A_N after re-watering ($7.0 \mu\text{mol CO}_2 \text{ m}^{-2} \text{ s}^{-1}$, Figure 2a), and this value was statistically significant different ($p < 0.05$, Table 1) when measured on well-watered plants ($10.9 \mu\text{mol CO}_2 \text{ m}^{-2} \text{ s}^{-1}$, Figure 2a). This fact can be explained by the low g_s after re-watering ($0.084 \text{ mol H}_2\text{O m}^{-2} \text{ s}^{-1}$, Figure 2b), i.e., much lower ($p < 0.05$, Table 1) than the value showed by well-watered plants ($0.288 \text{ mol H}_2\text{O m}^{-2} \text{ s}^{-1}$, Figure 2b). As a result, stomatal limitations to photosynthesis (l_s) increased significantly after re-watering when compared with the values estimated for both well-watered plants and during the drought period (Figure 4).

Table 1. Outputs of the Student's *t*-tests performed to compare the values of net photosynthesis (A_N), stomatal conductance (g_s), mesophyll conductance (g_m) and maximum velocity of carboxylation (V_{cmax}) for well-watered plants before the drought period and those measured 7 days after plants were rewatered. *: Significant values at $p < 0.05$.

	<i>t</i> -Value	<i>p</i> -Value
A_N	2.20	0.049 *
g_s	4.38	0.001 *
g_m	0.43	0.668
V_{cmax}	1.27	0.231

These apparently discrepancies between our results and those showed by Galle et al. [22] can be explained by considering the different levels of water stress reached when both studies are compared. Thus, midday water potential (ψ_{MD}) in holm oak only decreased to -2.9 MPa in Galle et al. [22], whereas in our study, ψ_{MD} was close to -6 MPa at the end of the drought cycle (Figure 5). These differences in ψ_{MD} between both experiments would have important consequences in terms of loss of xylem hydraulic conductivity. Effectively, we found that xylem embolism for holm oak twigs was ca. 50% at the end of the drought period, whereas ψ_{MD} reported by Galle et al. [22] would only induce an almost negligible level of xylem embolism—ca. 10%—according to our data and those previously published by Peguero-Pina et al. [19] for holm oaks of different provenances. The preservation of the integrity of xylem water transport may justify the rapid recovery of g_s found for holm oak by Gallé et al. [22] once water potential was restored to control values. In contrast, the meaningful value of xylem embolism and the lack of hydraulic recovery (Figure 5) could explain the strong down-regulation of g_s , even after re-watering, found in the our study.

The role of the hydraulic limitations in the recovery of leaf gas exchange once re-watered after a drought period has been discussed in previous studies [28,48,49]. Thus, Brodribb and Cochard [49] found strong evidence that hydraulic limitation was the process governing gas-exchange recovery

from drought in water stressed conifers. On the other hand, Blackman et al. [48] suggested that, besides hydraulic limitations, non-hydraulic factors such as ABA might also be involved in limiting the rate of stomatal reopening after re-watering in four woody angiosperm species native to Australia. More recently, Yan et al. [28] stated that the stomatal recovery in *Amorpha fruticosa* L. and *Robinia pseudoacacia* L. in the re-watered stage was mainly mediated by hydraulic factors, although they also suggested that non-hydraulic limitations might also be involved in the recovery of gas exchange in *R. pseudoacacia*.

In our case, there is considerable evidence that points toward the predominant role of the hydraulic-stomatal limitation model proposed by Brodribb and Cochard [49] in the lack of recovery of A_N found in holm oak. First, ABA concentrations after re-watering were very far from those measured during the drought period, especially with respect to the maximum values registered when the stomatal closure occurred (Figure 6). Second, as stated above, g_m and V_{cmax} completely recovered their original values for well-watered plants (Figure 3). Therefore, these non-hydraulic factors would not limit the recovery of photosynthetic activity of holm oak. On the other hand, the water potential drop between predawn and midday ($\psi_{MD} - \psi_{PD}$) after re-watering (ca. 1 MPa) was much lower than for well-watered plants (ca. 2 MPa), which suggests a down-regulation of plant transpiration (i.e., through low g_s) coupled with a reduced ability for water transport through the xylem to transpiring leaves (i.e., due to xylem embolism), according to the model proposed by Oren et al. [50]. In this regard, although several authors have reported a recovery of hydraulic capacity by embolism repair after re-watering (e.g., [20,51–53]), this seems not to be the case of holm oak, at least when reaching water potential values close to PLC₅₀.

5. Conclusions

Holm oak showed conservative water-use behavior when subjected to drought, mainly associated to an increase in ABA that triggered the stomatal closure. This fact, together with strong declines in g_m and V_{cmax} , severely limited the photosynthetic ability of this species under intense water stress. In spite of minimal water losses and its higher resistance to drought-induced cavitation, drought stress led to an almost complete stomatal closure, and xylem embolism rates close to PLC₅₀. The partial recovery of A_N found after re-watering was mainly due to hydraulic factors, which reduced g_s in order to prevent extensive xylem embolism under subsequent drought events that could compromise plant survival. Nevertheless, the occurrence of accumulative episodes of extreme drought may have a negative effect on the long-term performance of holm oak, due to a reduced ability for carbon gain.

Supplementary Materials: The following are available online at <http://www.mdpi.com/1999-4907/9/7/443/s1>, Figure S1: Mean and maximum diurnal VPD at the experimental site from June to September of 2017.

Author Contributions: All authors conceived and designed the experiments; J.J.P.-P., Ó.M.-H. and D.S.-K. performed the experiments; J.J.P.-P. and Ó.M.-H. analyzed the data; J.J.P.-P. wrote the initial draft of the paper; all authors contributed to the discussion of the results and to the writing of the final version of the manuscript.

Funding: This research was funded by Instituto Nacional de Investigación y Tecnología Agraria y Alimentaria (INIA) grant number RTA2015-00054-C02-01. Research of D. S. K. is supported by a DOC INIA-CCAA contract co-funded by INIA and European Social Fund (ESF).

Acknowledgments: Authors thank Ernesto Ruiz for his valuable work during the experiment.

Conflicts of Interest: The authors declare no conflict of interest. The founding sponsors had no role in the design of the study; in the collection, analyses, or interpretation of data; in the writing of the manuscript, and in the decision to publish the results.

References

1. Montserrat-Martí, G.; Camarero, J.J.; Palacio, S.; Pérez-Rontomé, C.; Milla, R.; Albuixech, J.; Maestro, M. Summer-drought constrains the phenology and growth of two co-existing Mediterranean oaks with contrasting leaf habit: Implications for their persistence and reproduction. *Trees* **2009**, *23*, 787–799. [CrossRef]
2. Flexas, J.; Diaz-Espejo, A.; Gago, J.; Gallé, A.; Galmés, J.; Gulías, J.; Medrano, H. Photosynthetic limitations in Mediterranean plants: A review. *Environ. Exp. Bot.* **2014**, *103*, 12–23. [CrossRef]

3. Lionello, P.; Malanotte-Rizzoli, P.; Boscolo, R.; Alpert, P.; Artale, V.; Li, L.; Luterbacher, J.; May, W.; Trigo, R.; Tsimplis, M.; et al. The Mediterranean climate: An overview of the main characteristics and issues. In *Mediterranean Climate Variability*; Lionello, P., Malanotte-Rizzoli, P., Boscolo, R., Eds.; Elsevier: Amsterdam, The Netherlands, 2006; pp. 1–26. ISBN 978-0-444-52170-5.
4. Gil-Peigrín, E.; Saz, M.A.; Cuadrat, J.M.; Peguero-Pina, J.J.; Sancho-Knapik, D. Oaks under Mediterranean-type climates: Functional response to summer aridity. In *Oaks Physiological Ecology. Exploring the Functional Diversity of Genus Quercus L.*; Gil-Peigrín, E., Peguero-Pina, J.J., Sancho-Knapik, D., Eds.; Springer International Publishing: Basel, Switzerland, 2017; pp. 137–193. ISBN 978-3-319-69099-5.
5. Peñuelas, J.; Sardans, J.; Filella, I.; Estiarte, M.; Llusà, J.; Ogaya, R.; Carnicer, J.; Bartrons, M.; Rivas-Ubach, A.; Grau, O.; et al. Assessment of the impacts of climate change on Mediterranean terrestrial ecosystems based on data from field experiments and long-term monitored field gradients in Catalonia. *Environ. Exp. Bot.* **2018**, *152*, 49–59. [[CrossRef](#)]
6. Busotti, F.; Ferrini, F.; Pollastrini, M.; Fini, A. The challenge of Mediterranean sclerophyllous vegetation under climate change: From acclimation to adaptation. *Environ. Exp. Bot.* **2014**, *103*, 80–98. [[CrossRef](#)]
7. Niinemets, Ü.; Keenan, T. Photosynthetic responses to stress in Mediterranean evergreens: Mechanisms and models. *Environ. Exp. Bot.* **2014**, *103*, 24–41. [[CrossRef](#)]
8. Gallé, A.; Haldimann, P.; Feller, U. Photosynthetic performance and water relations in young pubescent oak (*Quercus pubescens*) trees during drought stress and recovery. *New Phytol.* **2007**, *174*, 799–810. [[CrossRef](#)] [[PubMed](#)]
9. Peguero-Pina, J.J.; Morales, F.; Flexas, J.; Gil-Peigrín, E.; Moya, I. Photochemistry, remotely sensed physiological reflectance index and de-epoxidation state of the xanthophyll cycle in *Quercus coccifera* under intense drought. *Oecologia* **2008**, *156*, 1–11. [[CrossRef](#)] [[PubMed](#)]
10. Peguero-Pina, J.J.; Sancho-Knapik, D.; Morales, F.; Flexas, J.; Gil-Peigrín, E. Differential photosynthetic performance and photoprotection mechanisms of three Mediterranean evergreen oaks under severe drought stress. *Funct. Plant Biol.* **2009**, *36*, 453–462. [[CrossRef](#)]
11. Klein, T. The variability of stomatal sensitivity to leaf water potential across tree species indicates a continuum between isohydric and anisohydric behaviours. *Funct. Ecol.* **2014**, *28*, 1313–1320. [[CrossRef](#)]
12. Vilagrosa, A.; Bellot, J.; Vallejo, V.R.; Gil-Peigrín, E. Cavitation, stomatal conductance, and leaf dieback in seedlings of two co-occurring Mediterranean shrubs during an intense drought. *J. Exp. Bot.* **2003**, *54*, 2015–2024. [[CrossRef](#)] [[PubMed](#)]
13. Tombesi, S.; Nardini, A.; Frioni, T.; Socolini, M.; Zadra, C.; Farinelli, D.; Poni, S.; Palliotti, A. Stomatal closure is induced by hydraulic signals and maintained by ABA in drought-stressed grapevine. *Sci. Rep.* **2015**, *5*, 12449. [[CrossRef](#)] [[PubMed](#)]
14. McDowell, N.G. Mechanisms linking drought, hydraulics, carbon metabolism, and vegetation mortality. *Plant Physiol.* **2011**, *155*, 1051–1059. [[CrossRef](#)] [[PubMed](#)]
15. Hochberg, U.; Rockwell, F.E.; Holbrook, N.M.; Cochard, H. Iso/Anisohydry: A Plant-Environment Interaction Rather Than a Simple Hydraulic Trait. *Trends Plant Sci.* **2018**, *23*, 112–120. [[CrossRef](#)] [[PubMed](#)]
16. Hacke, U.G.; Sperry, J.S.; Pittermann, J. Drought experience and cavitation resistance in six shrubs from the Great Basin, Utah. *Basic Appl. Ecol.* **2000**, *1*, 31–41. [[CrossRef](#)]
17. Vilagrosa, A.; Morales, F.; Abadía, A.; Bellot, J.; Cochard, H.; Gil-Peigrín, E. Are symplast tolerance to intense drought conditions and xylem vulnerability to cavitation coordinated? An integrated analysis of photosynthetic, hydraulic and leaf level processes in two Mediterranean drought-resistant species. *Environ. Exp. Bot.* **2010**, *69*, 233–242. [[CrossRef](#)]
18. Aguadé, D.; Poyatos, R.; Rosas, T.; Martínez-Vilalta, J. Comparative drought responses of *Quercus ilex* L. and *Pinus sylvestris* L. in a montane forest undergoing a vegetation shift. *Forests* **2015**, *6*, 2505–2529. [[CrossRef](#)]
19. Peguero-Pina, J.J.; Sancho-Knapik, D.; Barrón, E.; Camarero, J.J.; Vilagrosa, A.; Gil-Peigrín, E. Morphological and physiological divergences within *Quercus ilex* support the existence of different ecotypes depending on climatic dryness. *Ann. Bot.* **2014**, *114*, 301–313. [[CrossRef](#)] [[PubMed](#)]
20. Martorell, S.; Diaz-Espejo, A.; Medrano, H.; Ball, M.C.; Choat, B. Rapid hydraulic recovery in *Eucalyptus pauciflora* after drought: Linkages between stem hydraulics and leaf gas exchange. *Plant Cell Environ.* **2014**, *37*, 617–626. [[CrossRef](#)] [[PubMed](#)]

21. Flexas, J.; Barbour, M.M.; Brendel, O.; Cabrera, H.M.; Carriquí, M.; Díaz-Espejo, A.; Douthe, C.; Dreyer, E.; Ferrio, J.P.; Gago, J.; et al. Mesophyll conductance to CO₂: An unappreciated central player in photosynthesis. *Plant Sci.* **2012**, *193–194*, 70–84. [[CrossRef](#)] [[PubMed](#)]
22. Galle, A.; Florez-Sarasa, I.; El Aououad, H.; Flexas, J. The Mediterranean evergreen *Quercus ilex* and the semi-deciduous *Cistus albidus* differ in their leaf gas exchange regulation and acclimation to repeated drought and re-watering cycles. *J. Exp. Bot.* **2011**, *62*, 5207–5216. [[CrossRef](#)] [[PubMed](#)]
23. Schwalm, C.R.; Anderegg, W.R.L.; Michalak, A.M.; Fisher, J.B.; Biondi, F.; Koch, G.; Litvak, M.; Ogle, K.; Shaw, J.D.; Wolf, A.; et al. Global patterns of drought recovery. *Nature* **2017**, *54*, 202–205. [[CrossRef](#)] [[PubMed](#)]
24. Resco, V.; Ewers, B.E.; Sun, W.; Huxman, T.E.; Weltzin, J.F.; Williams, D.G. Drought induced hydraulic limitations constrain leaf gas exchange recovery from drought after precipitation pulses in the C3 woody legume, *Prosopis velutina*. *New Phytol.* **2009**, *181*, 672–682. [[CrossRef](#)] [[PubMed](#)]
25. Brodribb, T.J.; Bowman, D.J.M.S.; Nichols, S.; Delzon, S.; Burlett, R. Xylem function and growth rate interact to determine recovery rates after exposure to extreme water deficit. *New Phytol.* **2010**, *188*, 533–542. [[CrossRef](#)] [[PubMed](#)]
26. Chen, J.W.; Zhang, Q.; Li, X.S.; Cao, K.F. Gas exchange and hydraulics in seedlings of *Hevea brasiliensis* during water stress and recovery. *Tree Physiol.* **2010**, *30*, 876–885. [[CrossRef](#)] [[PubMed](#)]
27. Guadagno, C.R.; Ewers, B.E.; Speckman, H.N.; Aston, T.L.; Huhn, B.J.; DeVore, S.B.; Ladwig, J.T.; Strawn, R.N.; Weinig, C. Dead or Alive? Using Membrane Failure and Chlorophyll a Fluorescence to Predict Plant Mortality from Drought. *Plant Physiol.* **2017**, *175*, 223–234. [[CrossRef](#)] [[PubMed](#)]
28. Yan, W.; Zheng, S.; Zhong, Y.; Shangguan, Z. Contrasting dynamics of leaf potential and gas exchange during progressive drought cycles and recovery in *Amorpha fruticosa* and *Robinia pseudoacacia*. *Sci. Rep.* **2017**, *7*, 4470. [[CrossRef](#)] [[PubMed](#)]
29. Rundel, P.W.; Jarrell, W.M. Water in the environment. In *Plant Physiological Ecology: Field Methods and Instrumentation*, 1st ed.; Percy, R.W., Ehleringer, J., Mooney, H.A., Rundel, P.W., Eds.; Chapman and Hall: London, UK, 1989; pp. 29–56. ISBN 978-0-412-40730-2.
30. Turner, N.C. Measurement of plant water status by pressure chamber technique. *Irrigation Sci.* **1988**, *9*, 289–308. [[CrossRef](#)]
31. Genty, B.; Briantais, J.M.; Baker, N.R. The relationship between the quantum yield of photosynthetic electron transport and quenching of chlorophyll fluorescence. *Biochim. Biophys. Acta* **1989**, *990*, 87–92. [[CrossRef](#)]
32. Krall, J.P.; Edwards, G.E. Relationship between photosystem II activity and CO₂ fixation in leaves. *Physiol. Plant.* **1992**, *86*, 80–187. [[CrossRef](#)]
33. Peguero-Pina, J.J.; Sisó, S.; Fernández-Marín, B.; Flexas, J.; Galmés, J.; García-Plazaola, J.I.; Niinemets, Ü.; Sancho-Knapik, D.; Gil-Pelegrín, E. Leaf functional plasticity decreases the water consumption without further consequences for carbon uptake in *Quercus coccifera* L. under Mediterranean conditions. *Tree Physiol.* **2016**, *36*, 356–367. [[CrossRef](#)] [[PubMed](#)]
34. Flexas, J.; Díaz-Espejo, A.; Berry, J.A.; Galmés, J.; Cifre, J.; Kaldenhoff, R.; Medrano, H.; Ribas-Carbó, M. Analysis of leakage in IRGA's leaf chambers of open gas exchange systems: Quantification and its effects in photosynthesis parameterization. *J. Exp. Bot.* **2007**, *58*, 1533–1543. [[CrossRef](#)] [[PubMed](#)]
35. Harley, P.C.; Loreto, F.; Di Marco, G.; Sharkey, T.D. Theoretical considerations when estimating the mesophyll conductance to CO₂ flux by the analysis of the response of photosynthesis to CO₂. *Plant Physiol.* **1992**, *98*, 1429–1436. [[CrossRef](#)] [[PubMed](#)]
36. De Kauwe, M.G.; Lin, Y.-S.; Wright, I.J.; Medlyn, B.E.; Crous, K.Y.; Ellsworth, D.S.; Maire, V.; Prentice, I.C.; Atkin, O.K.; Rogers, A.; et al. A test of the 'one-point method' for estimating maximum carboxylation capacity from field-measured, light-saturated photosynthesis. *New Phytol.* **2016**, *210*, 1130–1144. [[CrossRef](#)] [[PubMed](#)]
37. Flexas, J.; Ortuño, M.F.; Ribas-Carbó, M.; Díaz-Espejo, A.; Flórez-Sarasa, I.D.; Medrano, H. Mesophyll conductance to CO₂ in *Arabidopsis thaliana*. *New Phytol.* **2007**, *175*, 501–511. [[CrossRef](#)] [[PubMed](#)]
38. Grassi, G.; Magnani, F. Stomatal, mesophyll conductance and biochemical limitations to photosynthesis as affected by drought and leaf ontogeny in ash and oak trees. *Plant Cell Environ.* **2005**, *28*, 834–849. [[CrossRef](#)]
39. Tomás, M.; Flexas, J.; Copolovici, L.; Galmés, J.; Hallik, L.; Medrano, H.; Ribas-Carbó, M.; Tosens, T.; Vislap, V.; Niinemets, Ü. Importance of leaf anatomy in determining mesophyll diffusion conductance to CO₂ across species: Quantitative limitations and scaling up by models. *J. Exp. Bot.* **2013**, *64*, 2269–2281. [[CrossRef](#)] [[PubMed](#)]

40. Peguero-Pina, J.J.; Sisó, S.; Flexas, J.; Galmés, J.; García-Nogales, A.; Niinemets, Ü.; Sancho-Knapik, D.; Saz, M.Á.; Gil-Pelegrín, E. Cell-level anatomical characteristics explain high mesophyll conductance and photosynthetic capacity in sclerophyllous Mediterranean oaks. *New Phytol.* **2017**, *214*, 585–596. [[CrossRef](#)] [[PubMed](#)]
41. Pearcy, R.W.; Schulze, E.-D.; Zimmermann, R. Measurement of transpiration and leaf conductance. In *Plant Physiological Ecology: Field Methods and Instrumentation*, 1st ed.; Pearcy, R.W., Ehleringer, J., Mooney, H.A., Rundel, P.W., Eds.; Chapman and Hall: London, UK, 1989; pp. 137–160. ISBN 978-0-412-40730-2.
42. Cochard, H.; Breda, N.; Granier, A. Whole tree hydraulic conductance and water loss regulation in *Quercus* during drought: Evidence for stomatal control of embolism? *Ann. For. Sci.* **1996**, *53*, 197–206. [[CrossRef](#)]
43. Mayr, S.; Wieser, G.; Bauer, H. Xylem temperatures during winter in conifers at the alpine timberline. *Agric. For. Meteorol.* **2006**, *137*, 81–88. [[CrossRef](#)]
44. Sperry, J.S.; Donnelly, J.R.; Tyree, M.T. A method for measuring hydraulic conductivity and embolism in xylem. *Plant Cell Environ.* **1988**, *11*, 35–40. [[CrossRef](#)]
45. Sancho-Knapik, D.; Sanz, M.Á.; Peguero-Pina, J.J.; Niinemets, Ü.; Gil-Pelegrín, E. Changes of secondary metabolites in *Pinus sylvestris* L. needles under increasing soil water deficit. *Ann. For. Sci.* **2017**, *74*, 24. [[CrossRef](#)]
46. Peguero-Pina, J.J.; Sisó, S.; Flexas, J.; Galmés, J.; Niinemets, Ü.; Sancho-Knapik, D.; Gil-Pelegrín, E. Coordinated modifications in mesophyll conductance, photosynthetic potentials and leaf nitrogen contribute to explain the large variation in foliage net assimilation rates across *Quercus ilex* provenances. *Tree Physiol.* **2017**, *37*, 1084–1094. [[CrossRef](#)] [[PubMed](#)]
47. Munemasa, S.; Hauser, F.; Park, J.; Waadt, R.; Brandt, B.; Schroeder, J.I. Mechanisms of abscisic acid-mediated control of stomatal aperture. *Curr. Opin. Plant Biol.* **2015**, *28*, 154–162. [[CrossRef](#)] [[PubMed](#)]
48. Blackman, C.J.; Brodribb, T.J.; Jordan, G.J. Leaf hydraulics and drought stress: Response, recovery and survivorship in four woody temperate plant species. *Plant Cell Environ.* **2009**, *32*, 1584–1595. [[CrossRef](#)] [[PubMed](#)]
49. Brodribb, T.J.; Cochard, H. Hydraulic failure defines the recovery and point of death in water-stressed conifers. *Plant Physiol.* **2009**, *149*, 575–584. [[CrossRef](#)] [[PubMed](#)]
50. Oren, R.; Sperry, J.S.; Katul, G.G.; Pataki, D.E.; Ewers, B.E.; Phillips, N.; Schäfer, K.V.R. Survey and synthesis of intra- and interspecific variation in stomatal sensitivity to vapour pressure deficit. *Plant Cell Environ.* **1999**, *22*, 1515–1526. [[CrossRef](#)]
51. Brodersen, C.R.; McElrone, A.J.; Choat, B.; Matthews, M.A.; Shackel, K.A. The dynamics of embolism repair in xylem: In vivo visualizations using high-resolution computed tomography. *Plant Physiol.* **2010**, *154*, 1088–1095. [[CrossRef](#)] [[PubMed](#)]
52. Yang, S.; Tyree, M.T. A theoretical model of hydraulic conductivity recovery from embolism with comparison to experimental data on *Acer saccharum*. *Plant Cell Environ.* **1992**, *15*, 633–643. [[CrossRef](#)]
53. Salleo, S.; Lo Gullo, M.A.; De Paoli, D.; Zippo, M. Xylem recovery from cavitation-induced embolism in young plants of *Laurus nobilis*: A possible mechanism. *New Phytol.* **1996**, *132*, 47–56. [[CrossRef](#)]

